Plasmonics (2022) 17:1655–1660
https://doi.org/10.1007/s11468-022-01651-6

Photonic Quasi-Crystal Fiber-Based Plasmonic Biosensor: a Platform for Detection of Coronavirus

Mahsa Aliee[1] · **Mohammad Hazhir Mozaffari**[1]

Received: 23 February 2022 / Accepted: 25 April 2022 / Published online: 4 May 2022

Abstract

Since the coronavirus pandemic began, research groups worldwide developed diagnostic tests. One of the promising platforms for testing is an optical and plasmonic biosensor. Localized surface plasmon resonances owing to their highly concentrated field intensity provide highly sensitive devices. A beneficial approach to excite localized surface plasmon modes for field-based applications is using photonic crystal fibers while photonic quasi-crystals demonstrate a higher order of symmetry, the more isotropic Brillouin zone, and the easier achievement of photonic bandgap as compared with conventional photonic crystals. In this work, by exploiting a photonic quasi-crystal fiber, we are designing a surface plasmon resonance biosensor for the on-chip and real-time detection of coronaviruses. In our miniaturized design, a thin gold layer is employed on the outer layer of an air hole of a photonic quasi-crystal fiber with a 12-fold symmetry where the leakage of the fiber core mode can excite the surface plasmon resonance mode on the gold. According to three-dimensional finite-difference time-domain simulations, the proposed biosensor shows the sensitivity of 1172 nm/RIU in the detection of coronaviruses within the saliva. Moreover, the smallest detection limit obtained in the simulation is about 12 nm. These promising results altogether indicate that this reconfigurable and lab-on-a-chip platform can potentially be used in the detection of all kinds of coronaviruses.

Keywords Surface plasmon resonance · Photonic quasi-crystal fibers · Coronaviruses · Biosensors

Introduction

During the last two decades, high sensitivity in surface plasmon resonance (SPR) configurations causes to use of them as a reliable unique sensing platform based on photonic technology [1–3]. The first SPR sensor was fabricated in the 1980s for biological detection. Since the prism-based SPR sensors are bulky and have optical and mechanical components, they are not appropriate for field-based applications [4]; this drawback led to the development of the SPR sensor based on optical fibers in the 1990s. After that, various designs with various advantages and disadvantages are proposed for fiber-based SPR sensors. Among these designs, photonic crystal fiber (PCF)-SPR sensors due to their unique advantages such as the capability to be miniaturized, single-mode propagation, high-quality factor, and simplicity in light launching are attracting current interest. These advantages generally originate from their photonic bandgap (PBG) [5]. As PBG can be achieved in a quasi-periodic lattice, the photonic-quasi structures can open new frontiers for fiber-based SPR sensing technology. Importantly, thanks to the higher point group symmetry of the photonic-quasi crystals (PQC), their PBG is complete and shows more closely spherically symmetric as compared with PCs [6]. In other words, the higher order of symmetry, the more circular shape of the Brillouin, the more isotropic Brillouin zone, and the easier achievement of PBG for a refractive index contrast [7]. Because of the fact that PQCs are still in their infancy, PQC fiber (PQCF)-SPR devices have not been seriously proposed so far. Several designs for PQCF-SPR sensors were proposed such as selectively metal-coated [8, 9] using metallic slots [10], and photonic bandgap SPR sensors [11]. Lately, glycerol has been detected with a maximum sensitivity of 6000 nm/RIU by a ten-fold PQCF-based refractive index biosensor [12]. In 2017, a six-fold D-shaped PQCF biosensor was proposed; in this work, polymethyl methacrylate (PMMA) has been used as cladding in which the maximum refractive index sensitivity of 3200 nm/RIU was reported [13]. Two years later, Liu et al. presented a U-shaped PQCF

✉ Mohammad Hazhir Mozaffari
Mh.mozaffari@iausdj.ac.ir

[1] Department of Electrical Engineering, Sanandaj Branch, Islamic Azad University, Sanandaj, Iran

biosensor and with the help of gold and fluid infiltration, a maximum sensitivity of 33,600 nm/RIU was achieved [14], whereas, in 2021, they updated their work and increased sensitivity up to 42,000 nm/RIU [15]. Moreover, a PQCF-SPR sensor with indium tin oxide was designed with a sensitivity of 8750 nm/RIU [16]. The facilitating properties of the gold and the silver introduce them as the two most common materials used in SPR sensors that work at visible wavelengths. The resonance peak in silver is sharper than in gold and provides higher sensitivity, but high stability makes gold the ideal choice for SPR sensors [17–19]. The shape and location of thickness and dielectric constant of the metallic layer in the SPR absorption bands have been studied in several works [20–23]. PQCF plasmonic biosensors can detect the various type of DNA, bacteria, and virus [24, 25] and also different types of COVID-19 [26]. The sudden outbreak of COVID-19 in 2019 revealed the urgent need for fast and more reliable identification tools than before. Although computed tomography (CT) is widely used during this pandemic, it just can detect the signs of virus infection [27].

Based on the above observations, the main aim of this work is to design a PQCF-SPR device for on-chip and real-time detection of coronaviruses. In other words, a PQCF is exploited for exciting the highly concentrated SPR mode by which ultra-sensitivity can be achieved. Therefore, the leakage of the PQCF mode should cross the SPR mode of a gold thin layer. In our proposed design, a thin gold layer is deposited on the outer layer of an air hole of a PQCF with a 12-fold symmetry where the leakage of the fiber core mode can excite the SPR mode on the gold surface. Accordingly, a strong and highly confined SPR mode that can be exploited for our biosensing goals is realized.

Material and Methods

Proposed Structure

The cross-sectional image of the proposed platform is schematically depicted in Fig. 1. As shown, the PQCF lattice is provided a long-range 12-fold symmetry by using square-triangle tiling and random Stampfli inflation rule with a dodecahedral parent cell. This structure provides more isotropic and scattered light periodically by decreasing the orientational order of the system. In quasicrystal structures, air holes are randomly ensembled in squares and equilateral triangles. Resorting to the Stampfli inflation rule and large numbers of air holes in dodecahedral parent cells, we can achieve 12-fold symmetry. Air holes with 280 nm diameter are arranged at a 500 nm lattice distance. This solid-core PQCF is designed with the gold ring around one air hole in the first ring near the core which is shown in yellow color in Fig. 1. The diameters of this air hole and the gold ring are 250 and 300 nm, respectively. The PQCF can be fabricated by the sol–gel technique. The sol–gel casting technique is the unique method and independent technique of size and shape structures to modify and fabricate microstructure [28–30]. By using this method, air holes arrange well, and triangular or honeycomb lattices can easily generate. As mentioned before the use of gold can increase the sensor sensitivity while strong stability and larger shift at resonance peak make it an excellent choice. To analyze and simulate the device, the finite-difference time-domain (FDTD) method has been used [31].

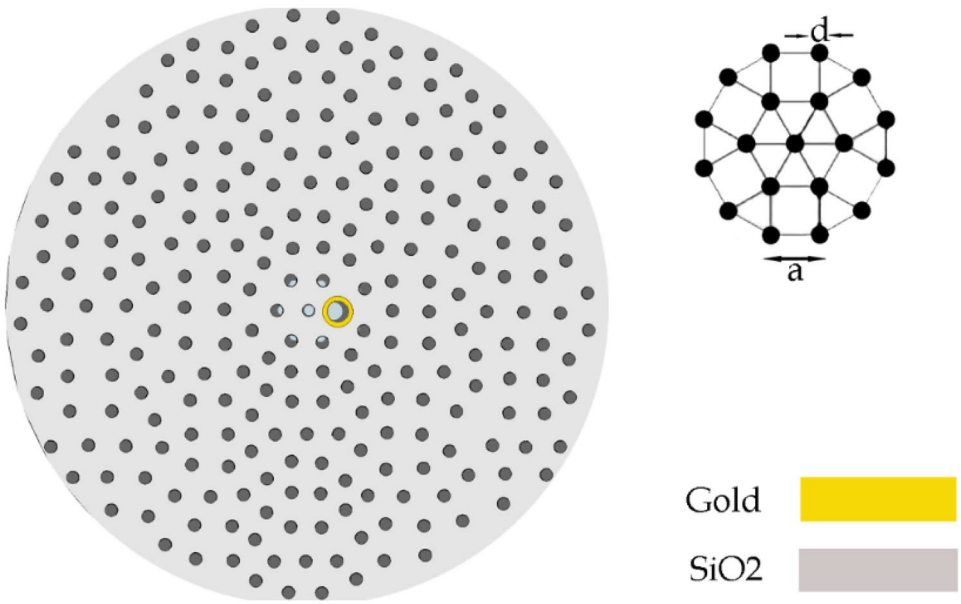

Fig. 1 The top-view illustration of the proposed device

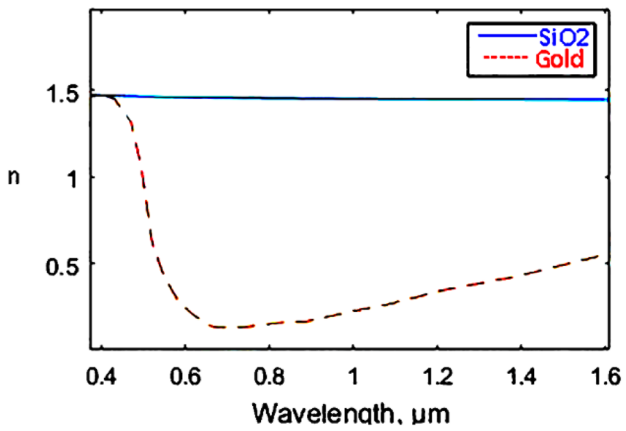

Fig. 2 Dispersion behavior of the material used in the simulation

Sensing Mechanism

This PQCF sensor has been designed for on-chip and real-time detection and analysis of different types of COVID-19 viruses. In our designed mechanism, the core mode of the fiber can excite the SPR within the gold-deposited hole; as a result, if the refractive index on that region changes, we will have a spectral shift in the output light that is gathered via a taper-fiber on the chip-surface. The existence of coronaviruses within the salvia changes its normal refractive index, providing the spectral shift as a sensing signal. It is worth noting that according to a recent study conducted by Kuppuswamy et al. [32] refractive indices of all types of Coronavirus (H5N1, H5N2, H9N2, H4N6, FAdV, and IBV) are within the negative ranges from " −0.96725

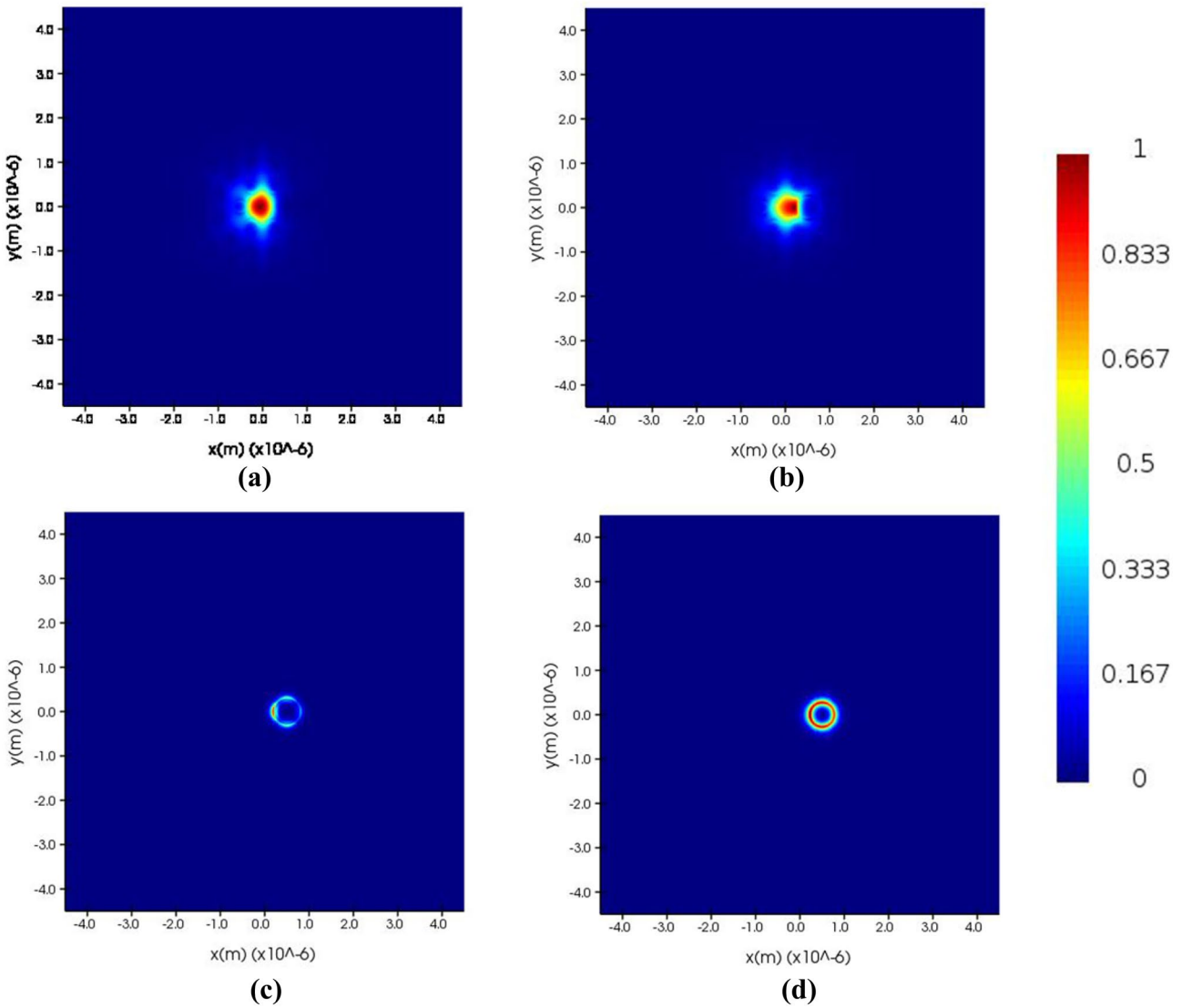

Fig. 3 Optical-electrical mode profiles of the proposed PQCF sensor: core mode profile (**a**), and the process of coupling between core mode and SPR mode (**b**-**d**)

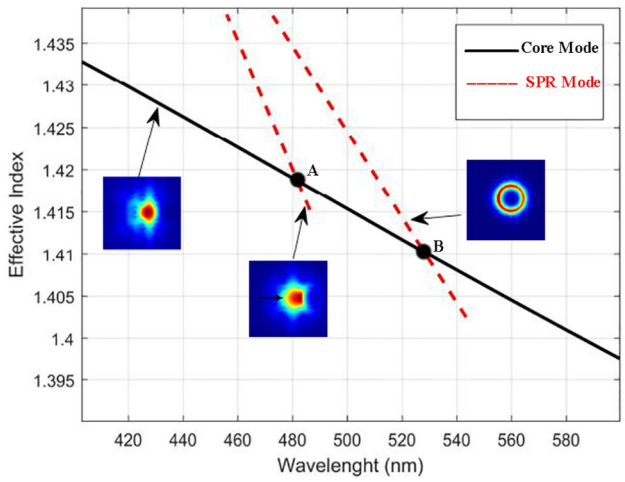

Fig. 4 The effective refractive index of the core mode and the SPR modes as a function of wavelength

to −0.999998." Also, Saliva refractive index has been experimentally calculated [33]. Samples are examined at 35 °C and wavelength range of 450–650 nm and represented index between 1.31 and 1.34.

Results and Discussion

The proposed device is analyzed through a 3D FDTD simulation method. In the simulation setup, we considered a Gaussian beam for exciting the designed fiber while a tapered fiber is employed for gathering the output light.

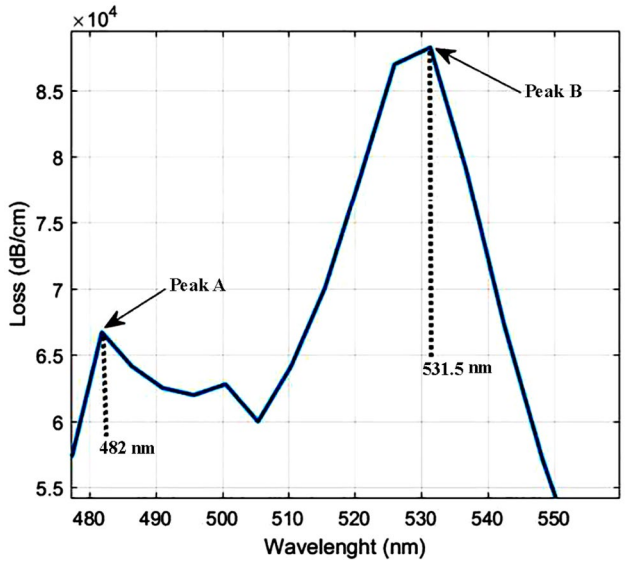

Fig. 5 Loss spectra of the core modes of the proposed PQCF-SPR biosensor

The refractive indices of the material used in this simulation are depicted in Fig. 2. Moreover, the boundary condition is anisotropic perfectly matched layers, and the mesh size is about 3 nm.

The optical-electrical field intensity within the proposed device at the wavelength of 532 nm is illustrated in Fig. 3. In Fig. 3a, one can see the core mode of the optical fiber. This good confinement is mainly achieved by the complete PBG of the quasi structure. The process of the coupling between core mode and SPR mode can be seen in Fig. 3b–d. As shown, the guided mode of the fiber can strongly couple with the SPR mode of the gold film deposited around a hole.

The SPR sensors work based on interactions of light with a metal surface and produce a quantum optical-electrical phenomenon. The light wavelength changes with a change in the refractive index of the sensing region. As soon as the excitation of the surface plasmon at the interface between a metal and a dielectric medium, the propagation constant of the surface plasmon changes. The sensing platform produces by coupling the energy of the core mode to the surface of the metal layer. Based on the mode-coupling theory, whenever the effective refractive index of the core mode and the SPR mode be equal (phase matching), they can couple to each other [34]. The real part of the refractive indices of the core mode and the SPR modes are shown in Fig. 4.

In this figure, dash red lines represent SPR modes in the coupling process, and a solid black line signifies the fundamental core mode. Moreover, the corresponding optical-electrical mode profile distributions of each mode are illustrated in their line. It is obvious that points A and B are phase matching points. To further investigation, we calculated the loss spectra of the core modes of the SPR sensor. The results are illustrated in Fig. 5. As can be seen in this figure, high losses happened when energy couples from core mode to the SPR mode in the related phase matching points. One can observe two phase matching take place in resonance wavelength at 482 nm and 532 nm. In addition, the maximum loss at the phase matching point plays an essential role in designing a PQCF-SPR. We choose point B with a wavelength of 532 nm as our work point.

As we know, the main parameter of a sensor is its sensitivity. To investigate the sensitivity of the proposed SPR-PQCF biosensor, we examine a situation in which a small amount of saliva is present inside the sensing region (gold-covered air hole) and made a comparison between normal saliva and saliva that contains coronaviruses providing the spectral characteristics in both cases. As stated before, the presence of the coronaviruses within the saliva changes its effective refractive index and leads to a spectral shift.

The effective refractive index of the fluid inserted in the air hole can be calculated as:

$$n_{\text{eff}} = \frac{n_{\text{s}} v_{\text{s}} + n_{\text{vi}} v_{\text{vi}}}{v_{\text{s}} + v_{\text{vi}}} \quad (1)$$

in which n_s and v_s are the refractive index and volume of the saliva and n_{vi} and v_{vi} are those for coronavirus. In our simulation, we calculated the effective refractive index of the sensing region via this equation and gathered the corresponding output peak for each case. The results are presented in Fig. 6 where the plot of output peak intensity versus the effective refractive index of the sensing region is depicted.

As calculated from this figure, the sensitivity of the proposed biosensor defined as $s \equiv |\Delta\lambda/\Delta neff|$ is about 1172 nm/RIU for the detection of coronaviruses that is well-comparable to state-of-the-art optical sensing platform [35–37]. This result indicates that the proposed on-reconfigurable platform can be considered as an alternative candidate for the conventional on-chip COVID-19 biosensors.

Another important parameter is the detection limit of a sensor. In our simulations, we modeled a sole coronavirus inside the saliva and changed its radius finding the minimum size of the virus that can cause a spectral shift. According to the simulation results, a single coronavirus with a radius as small as 12 nm can cause a 5.25-nm spectral shift that is well measurable and can be detected. In fact, this sensing limit is mainly achieved by the proposed miniaturized design in which a small change in the effective refractive index leads to a significant spectral blue shift. This detection shows an improvement as compared with similar photonic crystal-based biosensors [38–40]. It is worth noting that, simulation, in general, is constructed on the effective refractive index model to calculate the light–bio-analytes interactions, and hence, it is incapable of differentiating between two different viruses with similar refractive indices. This drawback can be overcome in the practical approaches by using bioreceptors [40].

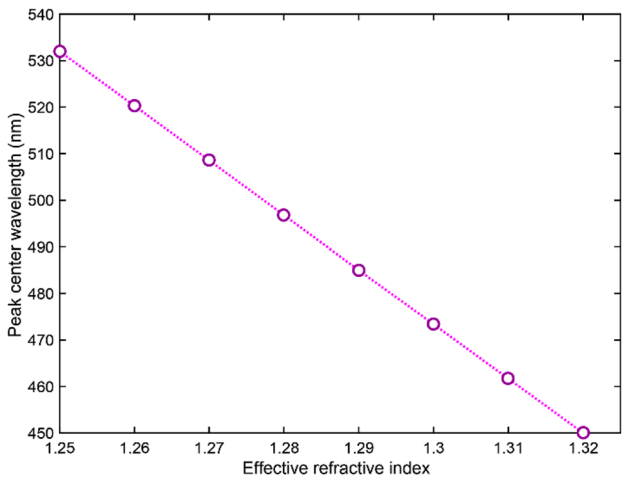

Fig.6. the plot of output peak intensity versus the effective refractive index of the sensing region

Conclusion

We have proposed a novel platform for the detection of coronaviruses that is reconfigurable, real-time, and lab-on-a-chip providing high sensitivity. The proposed design comprises a PQCF for exciting an SPR mode that shapes on the inner surface of a gold-coated air hole. This air hole acts as a sensing region of the device and due to its highly confined optical-electrical field intensity can sense any change that occurs in its effective refractive index. We have used 3D FDTD simulation to examine the device's capability in the detection of coronaviruses. These simulations indicate that the biosensor sensitivity is about 1172 nm/RIU which is well comparative to the modern SPR-based sensors. Moreover, the detection limit is as small as 12 nm. It is worth noting that this reconfigurable device can be readily redesigned and expanded to achieve more sensing area and for sensing larger biomolecules.

Author contribution Mahsa Aliee: software, data curation, investigation. Mohammad Hazhir Mozaffari: methodology, conceptualization, supervising, writing the paper. All authors discussed the results and contributed to the final manuscript.

Availability of data and material All data included in this paper are available upon request by contact with the contact corresponding author.

Code availability All codes included in this paper are available upon request by contact with the contact corresponding author.

Declarations

Ethics approval This is a theoretical work which is used for sensing platform.

Consent to participate Not applicable.

Consent for publication Not applicable.

Competing interests The authors declare no competing interests.

References

1. Homola J, Piliarik M (2006) Surface plasmon resonance (SPR) sensors In Surface Plasmon Resonance Based Sensors, J. Homola, Ed., ed Berlin, Heidelberg: Springer Berlin Heidelberg 45–67
2. Zangeneh AMR, Farmani A, Mozaffari MH, Mir A (2022) Enhanced sensing of terahertz surface plasmon polaritons in graphene/J-aggregate coupler using FDTD method. Diam Relat Mater 125:109005
3. Mozaffari MH (2022) Plasmon-enhanced optical tweezing systems: fundamental and applications. In Plasmon-enhanced light-matter interactions, P. Yu, H. Xu, and Z. M. Wang, Eds., ed Cham: Springer International Publishing, pp. 207–231

4. Yang XC, Lu Y, Wang MT, Yao JQ (2016) A photonic crystal fiber glucose sensor filled with silver nanowires. Opt Commun 359:279–284
5. Eivazi S, Mozaffari MH (2018) Numerical design and investigation of an optically pumped 1.55 μm single quantum dot photonic crystal-based laser. Photonics Nanostruct Fundam Appl 32:42–46
6. Man W, Megens M, Steinhardt PJ, Chaikin PM (2005) Experimental measurement of the photonic properties of icosahedral quasicrystals. Nature 436:993–996
7. Aliee M, Mozaffari MH, Saghaei H (2020) Dispersion-flattened photonic quasicrystal optofluidic fiber for telecom C band operation. Photonics Nanostruct Fundam Appl 40:100797
8. Yu X, Zhang Y, Pan S, Shum P, Yan M, Leviatan Y et al (2009) A selectively coated photonic crystal fiber based surface plasmon resonance sensor. J Opt 12:015005
9. Popescu VA (2013) A very high amplitude sensitivity of a new multi-core holey fiber-based plasmonic sensor. Mod Phys Lett B 27:1350038
10. Akowuah EK, Gorman T, Ademgil H, Haxha S, Robinson GK, Oliver JV (2012) Numerical analysis of a photonic crystal fiber for biosensing applications. IEEE J Quantum Electron 48:1403–1410
11. Gauvreau B, Hassani A, Fehri MF, Kabashin A, Skorobogatiy M (2007) Photonic bandgap fiber-based surface plasmon resonance sensors. Opt Express 15:11413–11426
12. Gandhi MSA, Sivabalan S, Babu PR, Senthilnathan K (2016) Designing a biosensor using a photonic quasi-crystal fiber. IEEE Sens J 16:2425–2430
13. Chu S, Kaliyaperumal N, Melwin G, Aphale SS, Kalivaradhan PEB, Karthikrajan S (2017) Designing a biosensor using a photonic quasi-crystal fiber with fan-shaped analyte channel. In Modeling, Design and Simulation of Systems, Singapore, pp. 529–537
14. Liu Q, Yan B, Liu J (2019) U-shaped photonic quasi-crystal fiber sensor with high sensitivity based on surface plasmon resonance. Appl Phys Express 12:052014
15. Liu Q, Jiang Y, Sun Y, Hu C, Sun J, Liu C et al (2021) Surface plasmon resonance sensor based on U-shaped photonic quasi-crystal fiber. Appl Opt 60:1761–1766
16. Liu Q, Sun J, Sun Y, Liu W, Wang F, Yang L et al (2019) Surface plasmon resonance sensor based on eccentric core photonic quasi-crystal fiber with indium tin oxide. Appl Opt 58:6848–6853
17. Kanso M, Cuenot S, Louarn G (2007) Roughness effect on the SPR measurements for an optical fibre configuration: experimental and numerical approaches. J Opt A Pure Appl Opt 9:586–592
18. Mokri K, Mozaffari MH, Farmani A (2022) Polarization-dependent plasmonic nano-tweezer as a platform for on-chip trapping and manipulation of virus-like particles. IEEE Trans Nanobiosci 21:226–231
19. Mokri K, Mozaffari MH (2019) Numerical design of a plasmonic nano-tweezer for realizing high optical gradient force. Opt Laser Technol 119:105620
20. Mitsushio M, Miyashita K, Higo M (2006) Sensor properties and surface characterization of the metal-deposited SPR optical fiber sensors with Au, Ag, Cu, and Al. Sens Actuators A Phys 125:296–303
21. Watanabe M, Kajikawa K (2003) An optical fiber biosensor based on anomalous reflection of gold. Sens Actuators B Chem 89:126–130
22. Sharma AK, Gupta DB (2007) Metal–semiconductor nanocomposite layer based optical fibre surface plasmon resonance sensor. J Opt A Pure Appl Opt 9:180–185
23. Zanganeh AMR, Farmani A, Mozaffari MH, Mir A (20222) Design optimization and fabrication of graphene/j-aggregate kretschmann-Raether devices for refractive index sensing using plasmon-induced transparency phenomena. Plasmonics 17:811–821
24. Moradiani F, Farmani A, Mozaffari MH, Seifouri M, Abedi K (2020) Systematic engineering of a nanostructure plasmonic sensing platform for ultrasensitive biomaterial detection. Opt Commun 474:126178
25. Farmani A, Soroosh M, Mozaffari MH, Daghooghi T (2020) Chapter 25 - Optical nanosensors for cancer and virus detections. In *Nanosensors for Smart Cities*, B. Han, V. K. Tomer, T. A. Nguyen, A. Farmani, and P. Kumar Singh, Eds., ed: Elsevier, pp. 419–432
26. Soler M, Scholtz A, Zeto R, Armani AM (2020) Engineering photonics solutions for COVID-19. APL Photonics 5:090901
27. Maddali H, Miles CE, Kohn J, O'Carroll DM (2021) Optical biosensors for virus detection: prospects for SARS-CoV-2/COVID-19. ChemBioChem 22:1176–1189
28. Bise RT, Trevor DJ (2005) Sol-gel derived microstructured fiber: fabrication and characterization. In OFC/NFOEC Technical Digest. Optical Fiber Communication Conference 3:3
29. Hamzaoui HE, Bouazaoui M, Capoen B (2020) Chapter 14 - Sol–gel materials for optical fibers. In Sol-Gel Derived Optical and Photonic Materials, A. Martucci, L. Santos, R. Estefanía Rojas Hernández, and R. Almeida, Eds., ed: Woodhead Publishing, pp. 315–346
30. Ghasemi H, Mozaffari MH, Moradian R (2022) Effects of deposition time on structural and optical properties of ZnS and ZnS/Au thin films grown by thermal evaporation0 Phys B Condens Matter 627:413616
31. Ghasemi H, Mozaffari MH (2021) A simple proposal to reduce self-heating effect in SOI MOSFETs. Silicon 13:4189–4198
32. Kuppuswamy S, Swain K, Nayak S, Palai G (2020) Computation of refractive indices of corona viruses through reverse calculation. Curr Opt Photonics 4:566–570
33. El-Zaiat SY (2003) Interferometric determination of refraction and dispersion of human blood-serum, saliva, sweat and urine. Opt Laser Technol 35:55–60
34. Gauvreau B, Hassani A, Fehri MF, Kabashin A, Skorobogatiy MA (2007) Photonic bandgap fiber-based surface plasmon resonance sensors. Opt Express 15:11413–11426
35. Mozaffari MH, Ebnali-Heidari M, Abaeiani G, Moravvej-Farshi MK (2018) Designing a miniaturized photonic crystal based optofluidic biolaser for lab-on-a-chip biosensing applications. Organ Electron 54:184–191
36. Mozaffari MH, Ebnali-Heidari M, Moravvej-Farshi MK (2019) A proposal for ultra-sensitive intensity-based biosensing via photonic crystal optofluidic biolaser. Laser Phys 29:035803
37. Mozaffari MH, Farmani A (2019) On-chip single-mode optofluidic microresonator dye laser sensor. IEEE Sens J 20:3556–3563
38. Wang C, Quan Q, Kita S, Li Y, Lončar M (2015) Single-nanoparticle detection with slot-mode photonic crystal cavities. Appl Phys Lett 106:261105
39. Shao L, Jiang X-F, Yu X-C, Li B-B, Clements WR, Vollmer F et al (2013) Detection of single nanoparticles and lentiviruses using microcavity resonance broadening. Adv Mater 25:5616–5620
40. Mozaffari MH, Ebnali-Heidari M, Abaeiani G, Moravvej-Farshi MK (2017) Photonic crystal optofluidic biolaser. Photonics Nanostruct Fundam Appl 26:56–61